arXiv:hep-ph/0211205v1 13 Nov 2002

Exploring Small Extra Dimensions at the Large Hadron Collider

B.C. Allanach[$], **K. Odagiri**[†], **M.J. Palmer**[‡], **M.A. Parker**[‡], **A. Sabetfakhri**[‡] and **B.R. Webber**[‡]

[$]*LAPTH, 8 Chemin de Bellevue, B.P. 110, Annecy -le-vieux, France 74941*
[†]*Theory Group, KEK, Oho 1–1, Ibaraki 305–0801, Japan*
[‡]*Cavendish Laboratory, University of Cambridge, Madingley Road, Cambridge,*
CB3 0HE, UK

ABSTRACT: Many models that include small extra space dimensions predict graviton states which are well separated in mass, and which can be detected as resonances in collider experiments. It has been shown that the ATLAS detector at the Large Hadron Collider can identify such narrow states up to a mass of 2080 GeV in the decay mode $G \to e^+e^-$, using a conservative model. This work extends the study of the e^+e^- channel over the full accessible parameter space, and shows that the reach could extend as high as 3.5 TeV. It then discusses ways in which the expected universal coupling of the resonance can be confirmed using other decay modes. In particular, the mode $G \to \gamma\gamma$ is shown to be measurable with good precision, which would provide powerful confirmation of the graviton hypothesis. The decays $G \to \mu^+\mu^-, W^+W^-, Z^0Z^0$ and jet–jet are measurable over a more limited range of couplings and masses. Using information from mass and cross-section measurements, the underlying parameters can be extracted. In one test model, the size of the extra dimension can be determined to a precision in length of 7×10^{-33} m.

Contents

1. Introduction

An exciting idea to be tested in high-energy collider experiments is the possible existence of narrow graviton resonances in the TeV energy range. Such resonances are predicted in models with small extra spatial dimensions. An example is the localized gravity model of Randall and Sundrum (RS) [1]. This model aroused great theoretical interest because it motivates the weak-Planck scale hierarchy via an exponentially suppressed warp factor in a non-factorisable geometry. Many possible extensions and elaborations of this type of theory are being discussed in the literature [2, 3, 4, 5, 6, 7, 8, 9, 10]. Problems with negative tension brane instability in the original RS model are solved in some other models. For example, placing the branes on fixed points of orbifolds projects out the negative energy modes [11].

An extra scalar with couplings on the branes can be used to naturally stabilise the brane separation [12]. Warped extra dimensions (with associated graviton resonances) have also been considered in the context of supersymmetry [13, 14, 15, 16]. Thus the discovery of TeV-scale graviton resonances remains a possibility that needs to be considered seriously in preparing for future collider experiments.

In [17], the detection of a narrow graviton resonance using the ATLAS detector at the Large Hadron Collider was considered. The main aim of that paper was to establish the discovery limit in the most favourable decay channel, $G \to e^+e^-$. A similar study for the CMS detector has since been reported [18]. In [17] the angular distribution of the lepton pair was also studied, and it was shown that the spin-2 nature of the resonance could be confirmed up to a mass somewhat below the discovery limit.

Apart from its unique spin, the most striking characteristic of the graviton is its universal coupling to all types of matter and gauge fields. In the present paper we consider the accuracy with which the couplings of a narrow graviton resonance to leptons, electroweak bosons, hadronic jets and Higgs bosons could be measured at the LHC. As in [17], we use the expected properties of the ATLAS detector as a guide to experimental limitations and the simplest RS model to characterise the resonance parameters, but our results should apply to other general-purpose detectors and to a broad class of models. We do, however, assume that all matter and gauge fields are confined to the physical brane and do not propagate into extra dimensions, thus excluding models of the type considered in [19, 20].

In the simple RS scenario, a 5-dimensional non-factorizable geometry is used, with two 3-branes of opposite tension. A graviton Kaluza-Klein spectrum is created, with a scale

$$\Lambda_\pi = \overline{M}_{Pl} e^{-kr_c\pi} \tag{1.1}$$

where $\overline{M}_{Pl}$ is the reduced effective 4-D Planck scale, r_c is the compactification radius of the extra dimension, and k is a scale of the order of the Planck scale. The geometrical exponential factor (the 'warp factor') generates TeV scales from fundamental Planck scales and hence motivates the weak-Planck hierarchy, if $kr_c \approx 12$.

The masses of the graviton resonances are given by

$$m_n = kx_n e^{-kr_c\pi} = x_n(k/\overline{M}_{Pl})\Lambda_\pi \tag{1.2}$$

where x_n are the roots of the Bessel function of order 1 ($x_n = 3.8317, 7.0156, 10.1735$ for $n = 1, 2, 3$). The massive graviton excitations couple with equal strength to the visible sector [21]. However, the higher modes being suppressed by the falling parton distribution functions, only the lightest mode is considered in this paper. This does not in any way affect the generality of the approach, as the analysis can be applied to any such resonances, including the higher modes, so long as the resonances are narrow and sufficiently separated from the other modes. This is in contrast to studies in which many excitations, each with small coupling, contribute to some scattering process [22, 23, 24, 25, 26]. For brevity, we refer to the first massive resonance, with mass $m_G = m_1$, as "the graviton".

In the RS model, the couplings of the graviton are given by $1/\Lambda_\pi$. The graviton mass is determined by the ratio $k/\overline{M}_{Pl}$. Our results are presented in the plane of m_G, Λ_π to

allow comparisons to be made with any model in this class. We have also defined a specific test model (identical to that used in [17]), with a value of $k/\overline{M}_{Pl} = 0.01$ (at the bottom of the range suggested in [21]), which according to [20] is on the edge of 95% exclusion for a first graviton excitation mass of less than 2000 GeV. Thus, we assign a low coupling constant to the graviton, and hence obtain a conservative estimate of the production cross section. This choice leads naturally to a narrow resonance. This test scenario is used to illustrate the potential physics reach in each decay channel. As already emphasised, the results derived do not depend on the validity of this particular scenario, but can be applied to any model giving rise to narrow well-spaced graviton resonances. For example, our results in Section 4 show that in a model with $k/\overline{M}_{Pl} = 0.1$ ($\Lambda_\pi = 10$ TeV), the discovery limit in the e^+e^- channel rises to 3.5 TeV, as a consequence of the increased production cross section. Values of $k/\overline{M}_{Pl} > 0.1$ are disfavoured on theoretical grounds because the bulk curvature becomes too large [20].

An event generator capable of simulating the production and decay of spin-2 resonances has been developed. This generator is now part of the standard HERWIG [27, 28] simulation package (versions 6.2 and later). The generated events are passed through the ATLAS fast simulation (ATLFAST [29]), in order to give a realistic description of detector resolution and efficiency.

In the following sections, the event generator is described (section 2), followed by studies of graviton decays to leptons (section 4), photons and massive vector bosons (section 5), hadronic jets (section 6), and Higgs bosons (section 7). Finally, the ability of the LHC to determine model parameters, including the length scale of the extra dimension, is discussed. Here again we use the simplest RS scenario for illustration.

2. The event generator

The implementation of the graviton resonance in the HERWIG event generator has been described in [17]. The graviton decays are treated as $2 \rightarrow 2$ processes, consisting of the two hard production subprocesses $q\bar{q} \rightarrow G$ and $gg \rightarrow G$, followed by the graviton decay. The relevant matrix elements were computed from the Feynman rules given in [30, 31]. Interference with Standard Model background processes is neglected. For the range of parameter values considered here, the resonance is so narrow that its observed width is determined by the detector resolution in all decay channels, and hence interference effects cancel in all observable distributions. Note, however, that the neglect of interference is not a good approximation for the broad resonances considered in [18].

The production cross-sections in [17] were calculated using the parton distribution functions (PDFs) of Owens [32], set 1.1. The present work uses the more recent MRST [33] PDFs. This change has no effect on the conclusions of [17].

The resulting graviton production cross section at the LHC for the test model is shown as a function of the graviton mass in Figure 1. The dashed curve shows the predictions for the 'central gluon' and 'high gluon' leading-order PDFs of [33]; the solid curve is for the average of these, which is the default PDF set for HERWIG version 6.3 [34]. This has been found to give the best agreement with recent next-to-leading order fits [35]. The dashed

curves give an indication of the uncertainty due to reasonable variation of the gluon PDF. We see that, even with our conservative choice of the coupling, for a graviton mass of 1.5 TeV the expected number of produced gravitons is about 5000 for an integrated luminosity of 100 fb^{-1}, falling to about 70 at a mass of 3 TeV.
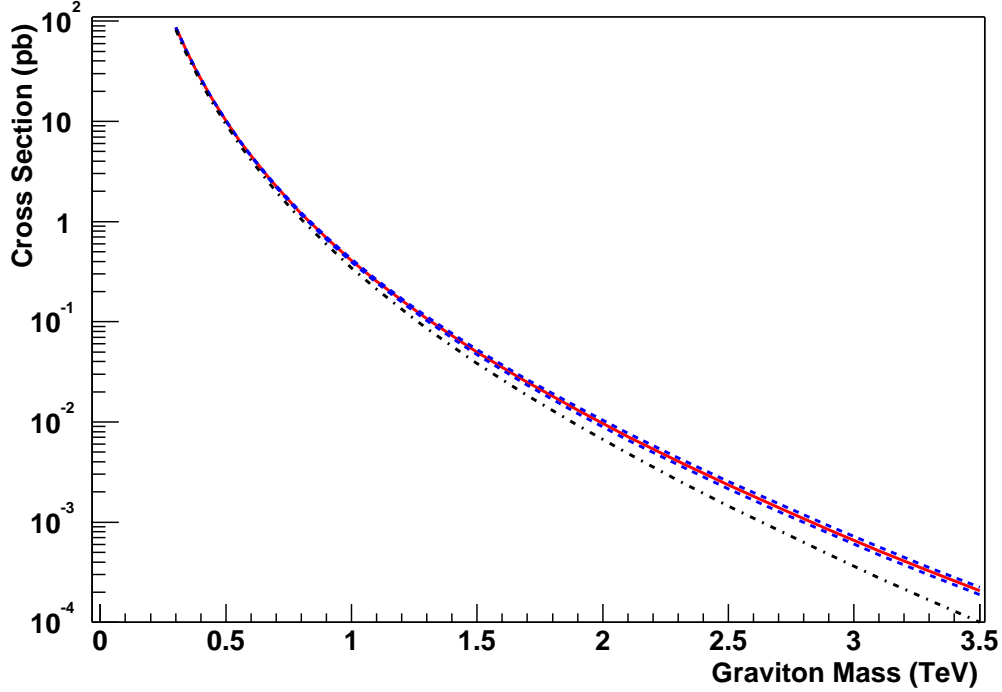

Figure 1: Cross section for graviton production at LHC.

The dot-dashed curve in Figure 1 shows the gluon fusion contribution to the cross section for the default PDF set; this is shown as a fraction of the total production cross section in Figure 2. Gluon fusion dominates the cross section for graviton masses up to 3.4 TeV. This has important implications for the angular distribution of the graviton decay (see below).

The branching fractions of the graviton into various decay modes are shown in Figure 3. These predictions are rather model-independent, depending only on the universality of the coupling. We see that decays into quark and gluon jets will predominate, due to their high multiplicity of colour, spin and flavour states. The Higgs boson fraction depends significantly on the assumed Higgs mass when $m_G < 10m_H$; we have used $m_H = 115$ GeV, the default HERWIG value. Out of 5000 produced gravitons with mass 1.5 TeV, we expect roughly 3500 jet-jet, 100 e^+e^-, 100 $\mu^+\mu^-$, 100 $\tau^+\tau^-$, 300 $\nu\bar{\nu}$, 200 $\gamma\gamma$, 450 W^+W^-, 225 Z^0Z^0 and 15 H^0H^0 decays.

The angular distributions of the various decay modes in the graviton rest frame are summarized in Table 1. Here β represents the velocity of the decay products, $\beta =$
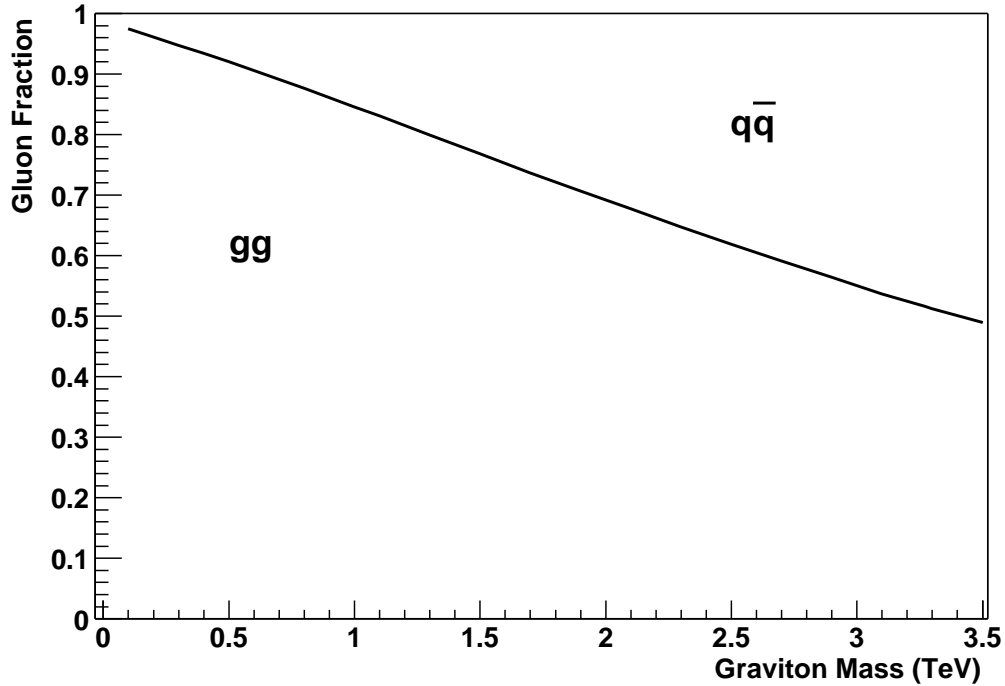
Figure 2: Contributions of gluon-gluon and quark-antiquark fusion to graviton production at LHC.

$\sqrt{1 - 4m^2/m_G^2}$ for particles of mass m. In Table 1, the plot letters refer to Figure 4, which shows the distributions in the limit of negligible mass ($\beta = 1$). Note that the angular distribution depends strongly on the production mechanism. As we saw above, gluon fusion predominates, but the contribution of quark-antiquark fusion has a structure that tends to flatten the decay angular distribution. Notice that the angular distributions of the massive gauge bosons W and Z are slightly different from those of the massless γ and gluon, even in the limit $\beta \to 1$, owing to their extra longitudinal polarization state, which has the same distribution as the Higgs boson.

3. Measurements of the graviton couplings

In [17] it was shown that the graviton resonance can be detected up to a mass of 2080 GeV in our test model, using the process $pp \to G \to e^+e^-$. The limits are model independent as long as the graviton couplings are universal and give rise to narrow resonances, with widths less than the experimental resolution. The angular distribution of the lepton pair can be used to determine the spin of the intermediate state. In our test model, the angular distribution favours a spin-2 hypothesis over a spin-1 hypothesis at 90% confidence for graviton masses up to 1720 GeV. In this work, we consider the full range of parameter space. In some cases, the search reach can be much higher than in the test model.
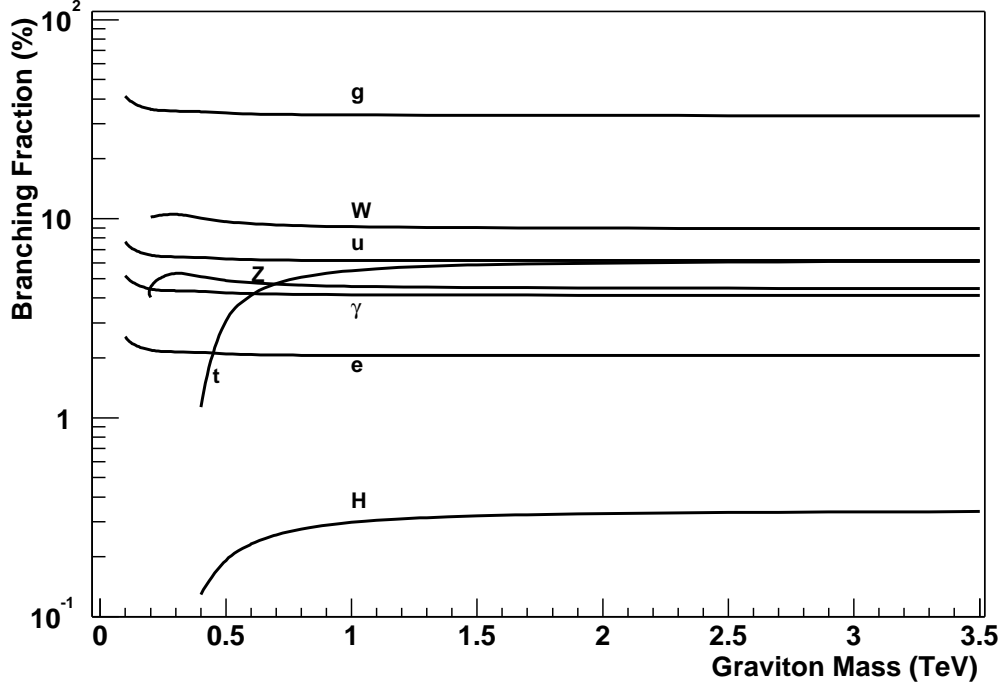
Figure 3: Graviton branching fractions.

Process	Distribution	Plot
$gg \to G \to f\bar{f}$	$\sin^2 \theta^* (2 - \beta^2 \sin^2 \theta^*)$	a
$q\bar{q} \to G \to f\bar{f}$	$1 + \cos^2 \theta^* - 4\beta^2 \sin^2 \theta^* \cos^2 \theta^*$	b
$gg \to G \to \gamma\gamma, gg$	$1 + 6\cos^2 \theta^* + \cos^4 \theta^*$	c
$q\bar{q} \to G \to \gamma\gamma, gg$	$1 - \cos^4 \theta^*$	a
$gg \to G \to WW, ZZ$	$1 - \beta^2 \sin^2 \theta^* + \frac{3}{16}\beta^4 \sin^4 \theta^*$	d
$q\bar{q} \to G \to WW, ZZ$	$2 - \beta^2(1 + \cos^2 \theta^*) + \frac{3}{2}\beta^4 \sin^2 \theta^* \cos^2 \theta^*$	e
$gg \to G \to HH$	$\sin^4 \theta^*$	f
$q\bar{q} \to G \to HH$	$\sin^2 \theta^* \cos^2 \theta^*$	g

Table 1: Angular distributions in graviton production and decay. θ^* is the polar angle of the outgoing fermion in the graviton rest frame. The letters in the "plot" column refer to the curves in Figure 4.

In the following, it is assumed that the graviton will be detected in the $e^+ e^-$ channel, with a significance of greater than 5σ. This study then assumes that the graviton mass is known, which allows signals with significances as low as 3σ to be used in the determination of the couplings.
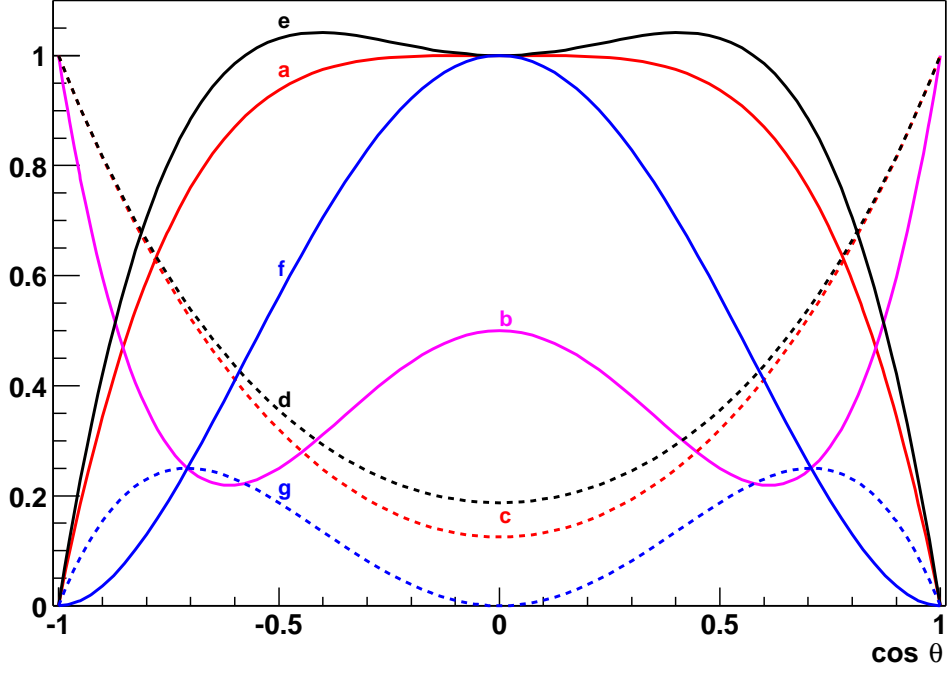
Figure 4: Angular distributions in graviton production and decay ($\beta = 1$).

4. Graviton decays to leptons

4.1 $G \to e^+ e^-$

This channel offers the best chance of discovery of a graviton resonance at the LHC, by virtue of the relatively small background from Drell-Yan processes, and the excellent mass resolution provided by the ATLAS electromagnetic calorimeter. More details of the proposed discovery search can be found in [17].

Measurements of the graviton coupling were studied by simulating signals at graviton masses between 0.5 and 4.0 TeV. These signals were superimposed on the expected background from Drell-Yan. Electrons were selected with $p_T > 5$ GeV inside the acceptance of the ATLAS tracking detector ($|\eta| < 2.5$), using the standard electron reconstruction algorithm of ATLFAST, which accounts for the effect of nearby particles on the calorimeter signature. The pair with the highest p_T were used to construct the graviton mass. The mass distribution of the electron pair is well fitted by a Gaussian signal on a background of the form $\alpha m_{ee}^{-\beta}$, where m_{ee} is the mass of the electron pair, and α and β are free parameters. The acceptance of the detector varies from 91 to 76% across the mass range, with an estimated systematic error of $< 1\%$, and a negligible statistical error. The efficiency for detecting an isolated electron is taken as 90%. The systematic error on this value will depend on the details of the detector and reconstruction code used, and is hence beyond the scope of this study. However, we note that, for the very high energy electrons involved

in these decays, it will not be necessary to make tight cuts on the electron tracks, and so a high efficiency with a small error should be obtained. The fit for a graviton mass of 1500 GeV is shown in Figure 5.
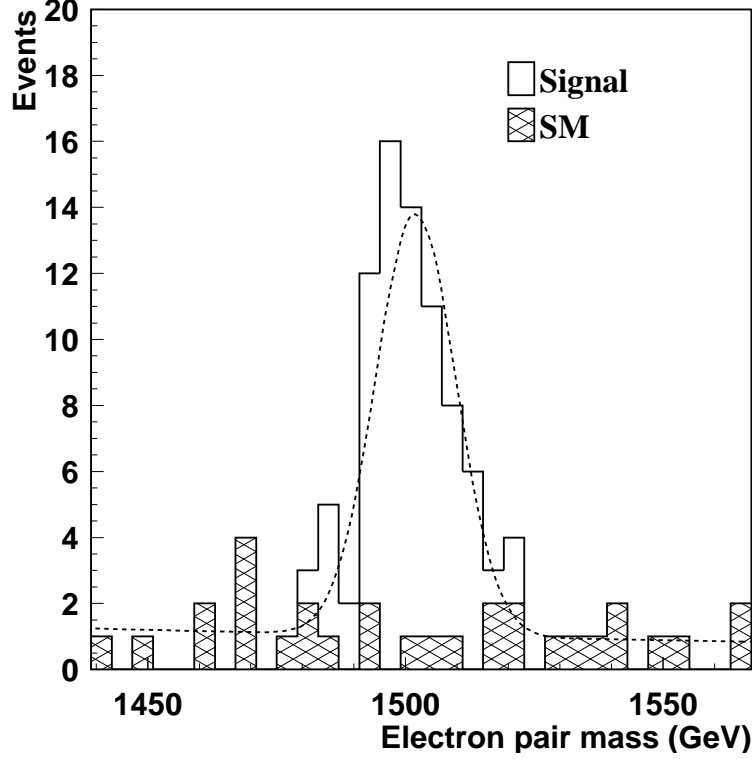

Figure 5: The number of events per 4 GeV mass bin from a graviton resonance, with $m_G = 1.5$ TeV (signal), superimposed on the expected Standard Model background (SM), for 100 fb^{-1} of integrated luminosity. The fit to the data is shown by the dotted curve.

In order to estimate the precision which could be expected for the measurement of the production cross-section times branching ratio $\sigma.B$, a procedure for subtracting the background under the peak is required. To avoid assumptions about the background shape, we use a simple background subtraction procedure. The background estimate N_B^{est} is obtained by counting the number of events in two bins of width $w/2$ on either side of the signal. This procedure will work well since the mass window used to select the signal, of width w, is narrow. It contains N events, made up of N_S signal and N_B background events. The error on the signal estimate N_S^{est} is then given by

$$\Delta N_S^{est} = \sqrt{\Delta N^2 + \Delta N_B^{est\ 2}} \ . \tag{4.1}$$

The fractional error on $\sigma.B$ is then simply equal to $\Delta N_S^{est}/N_S^{est}$

In a real experiment, it would be possible to use a more sophisticated procedure to obtain N_B^{est}, by fitting over a larger range of electron pair mass. This means that our estimates of the experimental reach are conservative. But since, in the interesting regions, the background levels are small, the effect of background subtraction on the final error is also small.

A systematic error arises from the errors on the acceptance, electron identification efficiency and luminosity. The method for luminosity measurement in ATLAS is not yet decided, but an error of 5-10% is within reach of conventional methods [36]. Methods to improve this to 1-2% are under consideration. Together with the as yet unknown electron reconstruction efficiency (see above) this means that the systematic error on cross-section measurements is very uncertain at present, and hence we plot our results using statistical errors only. The effect of the systematic error on the extraction of model parameters is discussed in section 9.

The above procedure was used to determine how well the ATLAS detector could measure the graviton coupling. The HERWIG/ATLFAST simulation was run at each graviton mass, and for the standard model background, for 100 fb^{-1} of integrated luminosity, corresponding to one year of running of the LHC at its nominal luminosity of 10^{34} cm^{-2}s^{-1}. The estimated statistical errors on $\sigma.B$ are plotted on Figure 6. Also shown are the region excluded by Tevatron data [37, 38] and lines of constant $k/\overline{M}_{Pl}$. In the test model, with $k/\overline{M}_{Pl} = 0.01$, a 10% measurement of the production rate is possible for graviton resonance masses as high as 1400 GeV. In models with $k/\overline{M}_{Pl} = 0.1$ ($\Lambda_{\pi} = 10$ TeV), a 20% measurement of the coupling is possible for graviton masses as high as 3.5 TeV, indicating the ultimate search reach. For completeness, we have continued the contours into the region of very small $k/\overline{M}_{Pl}$. This region is excluded in the RS–I model [20], but may be relevant to other models with low mass graviton resonances. In such a case, values of Λ_{π} as high as 100 TeV are in principle accessible. For high values of $k/\overline{M}_{Pl} > 0.05$, horizontally-striped on the plot, the graviton resonance width becomes larger than the experimental mass resolution, making a measurement of the width possible. It is unlikely that such a measurement would be possible in any of the other channels considered here, since their mass resolutions are far inferior. Once the width becomes very large, it would be necessary to increase the size of the mass window in order to maintain a high efficiency for the signal. Interference with the Drell-Yan background would also need to be taken into account. However, the production cross-section is proportional to $(k/\overline{M}_{Pl})^2$, and so the detection of the resonance is trivial in this region.

4.2 $G \to \mu^+\mu^-$

The analysis of this channel is very similar to that for the electron case. Muons were selected with $p_T > 5$ GeV using the standard muon reconstruction algorithm of ATLFAST. The pair with the highest p_T were used to construct the graviton mass. The discovery potential in the $\mu^+\mu^-$ channel is not as great as in the e^+e^- case, because the momentum resolution of the magnetic spectrometer decreases at high muon momentum. This is reflected in a much poorer mass resolution for high muon pair masses. In addition, the reconstruction efficiency is poorer than for electrons. Nonetheless, precisions of $\sigma.B < 10\%$ are achievable in the test model case, for graviton resonance masses up to 1250 GeV. Figure 7 shows the results, which can provide a valuable check of lepton universality in the graviton couplings.

4.3 $G \to \tau^+\tau^-$

The $\tau^+\tau^-$ decay mode would be extremely hard to observe on the large standard model
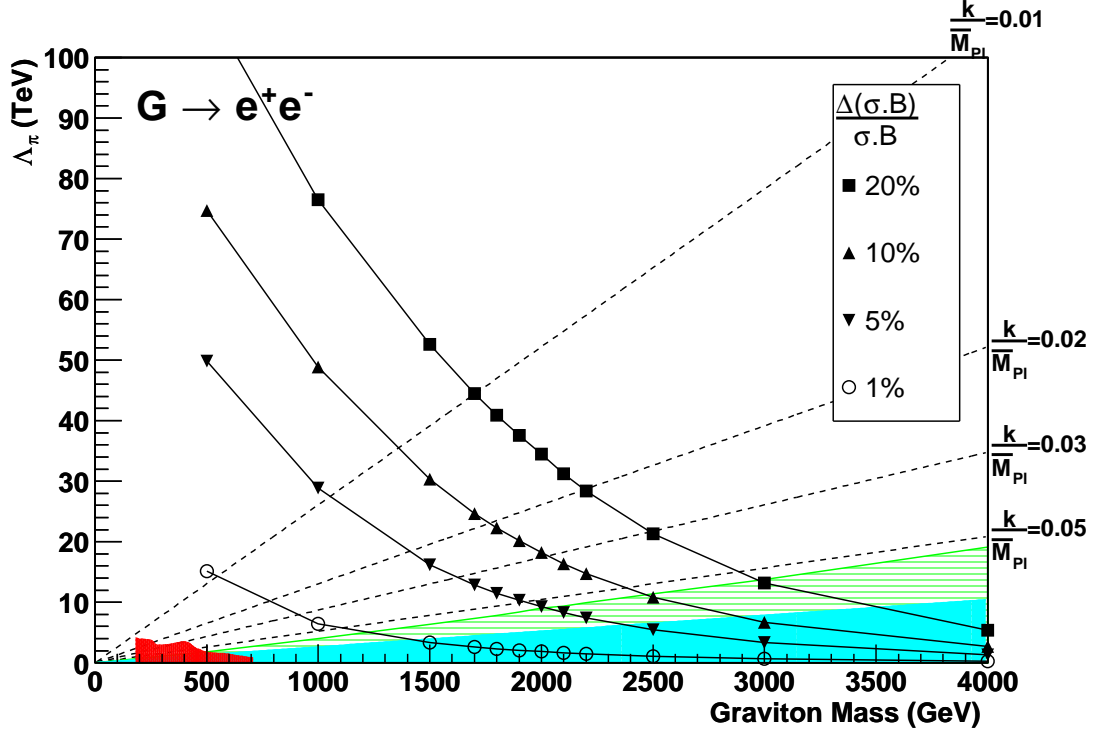
Figure 6: Contours showing the statistical precision expected for a measurement of $\sigma.B$ in the decay mode $G \rightarrow e^+e^-$ for 100 fb^{-1} of integrated luminosity (Solid lines with markers). Also shown are lines of equal $k/\overline{M}_{Pl}$ (dashed). The test model has $k/\overline{M}_{Pl} = 0.01$. The (red) blocked region near the origin is excluded by Tevatron data [37, 38]. In the (green) horizontally-striped region above $k/\overline{M}_{Pl} \approx 0.05$ the resonance width is larger than the experimental resolution. The (blue) blocked region with $k/\overline{M}_{Pl} > 0.1$ is disfavoured theoretically.

background from QCD jets. The missing energy from the τ decays would spoil the mass resolution for the graviton signal, further degrading the significance of any peak. This signal is therefore not considered further.

5. Decays to vector bosons

The detection of decays to vector bosons would be very important in establishing the nature of a graviton resonance, since the universal coupling would be very different from that expected for other exotic objects, such as a Z'. In addition the angular distribution of the decay products is a characteristic signature of the resonance spin (see Table 1 and Figure 4).

5.1 $G \rightarrow \gamma\gamma$

The method used to study this channel is identical to that used for the electron case. The minimum photon p_T was set to 1 GeV. A photon detection efficiency of 90% was applied after the effect of the standard photon selection cuts in ATLFAST.
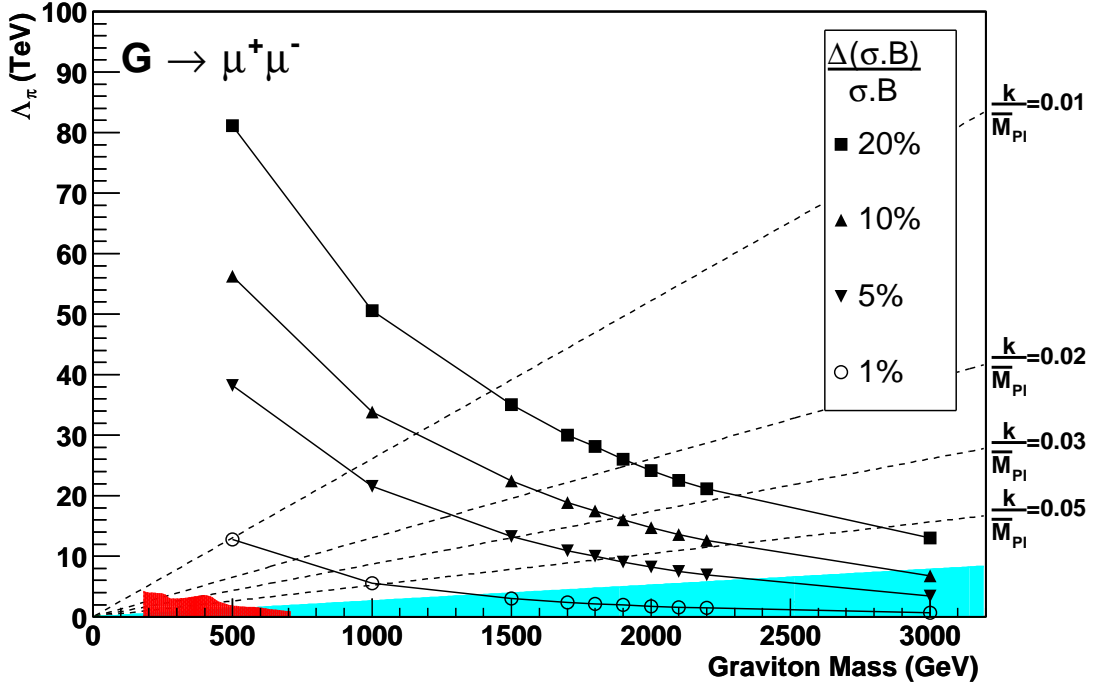
Figure 7: Contours showing the statistical precision expected for a measurement of $\sigma.B$ in the decay mode $G \to \mu^+\mu^-$ for 100 fb^{-1} of integrated luminosity, as for Figure 6.

The mass resolution for photon pairs is excellent, being very close to that for electrons. However the background is much less well understood. The HERWIG calculation of the cross-section only includes the Born term and production from gluon-gluon interactions via a quark box diagram. It is known that these diagrams alone predict a cross-section for photon pair production at the Tevatron which is a factor of ≈ 5 too small [39]. This large discrepancy means that one cannot rely on existing Monte Carlo simulations to produce a reliable background estimate, and in particular that the angular distribution of the background cannot be trusted. We note that these effects were not considered in [40].

As discussed in Section 2, graviton production at accessible masses is dominated by gluon-gluon fusion, and therefore the photon angular distribution is strongly forward-backward peaked, as shown by curve c in Figure 4. An important background, not presently simulated by HERWIG (or any other current event generator), is bremsstrahlung from initial state partons, which is also strongly forward-backward peaked. For these reasons, we do not attempt an analysis of how well the resonance spin could be determined at the LHC. However, it should be noted that the background level and angular distribution can easily be measured in the experiment by using data away from the resonance itself. The photon channel will then be very significant in establishing the nature of the resonance.

For this analysis, we use a photon pair background 5 times as large as predicted by HERWIG in order to estimate the precision which could be reached on the coupling in this
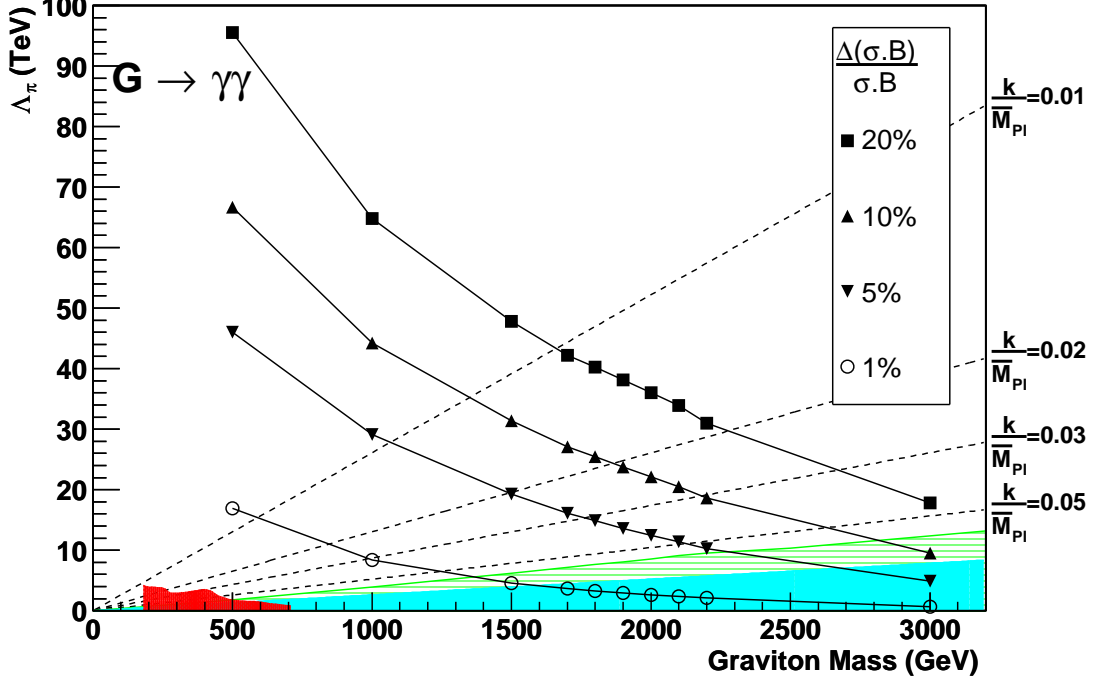
channel. The results are shown in Figure 8.

Figure 8: Contours showing the statistical precision expected for a measurement of $\sigma.B$ in the decay mode $G \to \gamma\gamma$ for 100 fb^{-1} of integrated luminosity, as for Figure 6.

5.2 $G \to WW \to l\nu jj$

Graviton decays to a pair of W bosons are best detected in the mode where one W decays leptonically to the electron or muon final states, and one hadronically. This mode has a reasonable branching fraction (29% of W pairs), and the reconstruction of the events can be performed by assuming that the missing energy is due only to the neutrino from the leptonic decay and using the W mass as a constraint.

This channel has considerable difficulties compared to the leptonic and $\gamma\gamma$ channels due to the large background from $t\bar{t}$ and $W+2$ jets. Consequently this channel would not be a discovery channel, but would be useful in confirming the universality of the graviton's coupling. Scale factors for the background were obtained by comparing the HERWIG cross-section with the NLL cross-section for $t\bar{t}$ [41] and by using the prescription in [42] for $W+2$ jets, giving scale factors of 1.8 and 1.7 respectively. Background from WW production was also included for completeness but was negligible compared to the other backgrounds.

Standard ATLFAST settings for high luminosity were used except for the jet reconstruction algorithm, for which the Mulguisin algorithm [43] with a minimum distance of $\Delta R = 0.2$ was used. This algorithm was chosen because it was found to give the highest signal reconstruction efficiency.

Jet reconstruction is problematic because the jets come from a W which is highly boosted. This naturally leads to two jets very close in $\eta - \phi$: for a 3 TeV graviton, both jets often fall within the same calorimeter cell as defined by ATLFAST.

The neutrino 4-momentum is reconstructed from $\not{E}_T$ and fixing the mass of the $l\nu$ system to be the mass of a W. This gives a quadratic equation which is solved and the average of the two solutions taken. The second W is reconstructed from the highest p_T jet and a jet which gives $65 < M_{jj} < 85$ GeV. If more than one possibility is found, the combination that gives the highest $p_T(W)$ is chosen.

The p_T cuts are set fairly low to allow the whole range of graviton masses above 500 GeV to be treated in a single analysis. Some improvement could be made by tuning these cuts for a smaller mass region, using the mass of the resonance as measured in the e^+e^- channel as a guide.

To reduce the $t\bar{t}$ background the following cuts were imposed: a top reconstruction veto which attempts to reconstruct a top mass from each of the Ws and an acceptably close jet (within $\Delta R < 1$), and a cut on the number of central ($|\eta| < 2$) jets.

The signal reconstruction efficiency is 22% at 1.5 TeV, dropping to 6% at 3 TeV. The mass resolution is 6%. The background is not well described by any simple form over the entire range, but it is very smooth. Therefore it is expected that background subtraction will be successfully achieved by fitting a function in the sidebands. The error on the background estimate was found by fitting an exponential with a window of $m \pm 2\sigma$ in a fit region $m \pm 6\sigma$. Figure 9 shows the background subtraction procedure, in the case $k/\overline{M}_{Pl} = 0.05$.

The error on the signal estimate, N_S^{est} is given by equation (4.1), taking the error on N_B^{est} to be the statistical error on the number of events in the fit region. The estimated statistical errors for $\sigma.B$ were then calculated in the same way as the other channels and are shown in Figure 10.

In the test model with $k/\overline{M}_{Pl} = 0.01$, a measurement of $\sigma.B$ is not possible. However, for higher values of $k/\overline{M}_{Pl}$, measurement is possible with statistical accuracies in the range 5-30%. For high masses, the overlap of jets means that the efficiency of the selection cuts becomes very low. A different analysis would be required, perhaps based on event shapes in order to extend the reach further. At low masses, the effects of the p_T cuts on the determination of the fit parameters can be seen.

5.3 $G \rightarrow ZZ \rightarrow lljj$

This channel is analyzed in much the same way as the WW channel. The principal difference is that the dominant background is $Z+2$ jets – there is no $t\bar{t}$ equivalent. Consequently, similar reconstruction and cuts were employed with the omission of the cuts intended to reduce the $t\bar{t}$ background.

The same background fitting and subtraction procedure as in the WW case is followed leading to a similar error determination, the results of which are shown in Figure 11.

Signal reconstruction efficiency is similar to the WW case and mass resolution is better, $\sim 3\%$. The smaller branching ratio for this decay is offset by the lower background and the
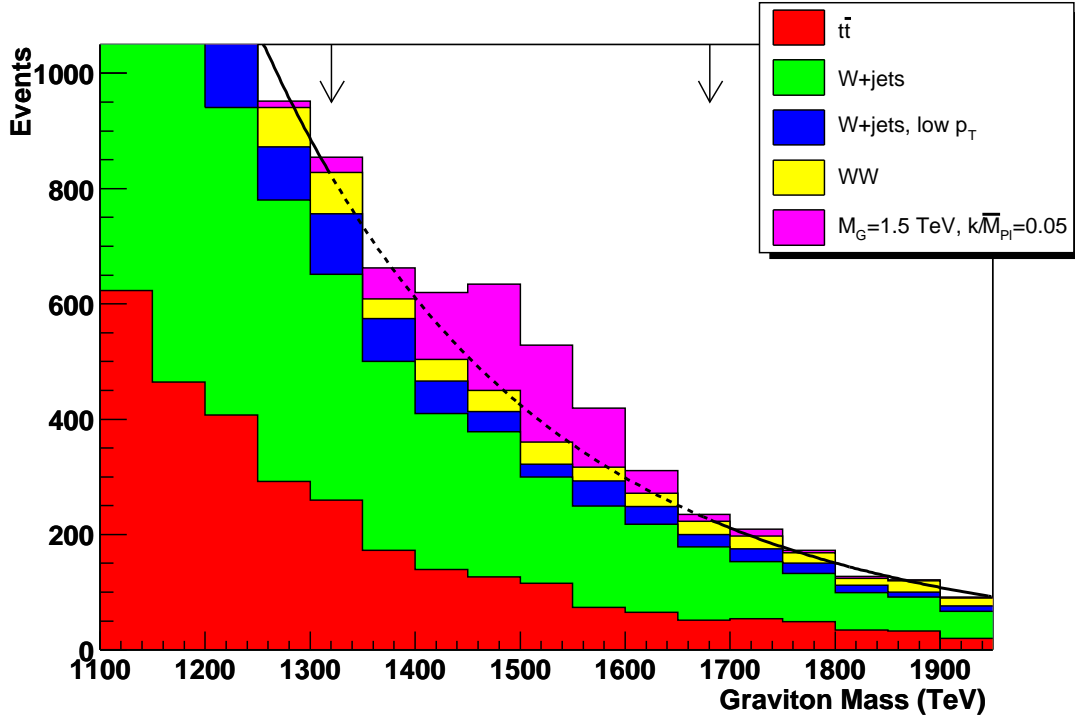
Figure 9: A fit to the background in the sidebands around the $G \to WW$ signal (solid line) and its extrapolation under the signal peak (dashed line).

final reach is very similar to the WW case. As before, the effect of decreasing efficiency at high mass is evident as is the effect of the p_T cuts at lower masses.

6. Decays to hadronic final states

6.1 Inclusive decays to 2 jets

The signature for the decay mode $G \to jj$ comprises two energetic jets in the detector, producing a large transverse hadronic energy. The dominant background process to this topology is QCD multi-jet production, which forms a continuum irreducible background. This large background would make it impossible to find a statistically significant signal peak without the knowledge of the peak position provided by other channels such as the e^+e^- final state, except in cases with very large graviton couplings. However, as stated above, we assume that any discovery will be made in other channels, and investigate the potential to measure the coupling strength alone in hadronic channels.

$G \to jj$ candidates are selected by requiring at least two jets with minimum transverse energies (E_T) of a quarter of the graviton mass. The continuum background is shown in Figure 12a, with a resonance at 1500 GeV superimposed, using $k/\overline{M}_{Pl} = 0.08$. The signal is not visible to the eye. The overall acceptance for the signal selection cuts ranges from 40% to 60% depending on the model parameters m_G and Λ_π. Although the signal observability
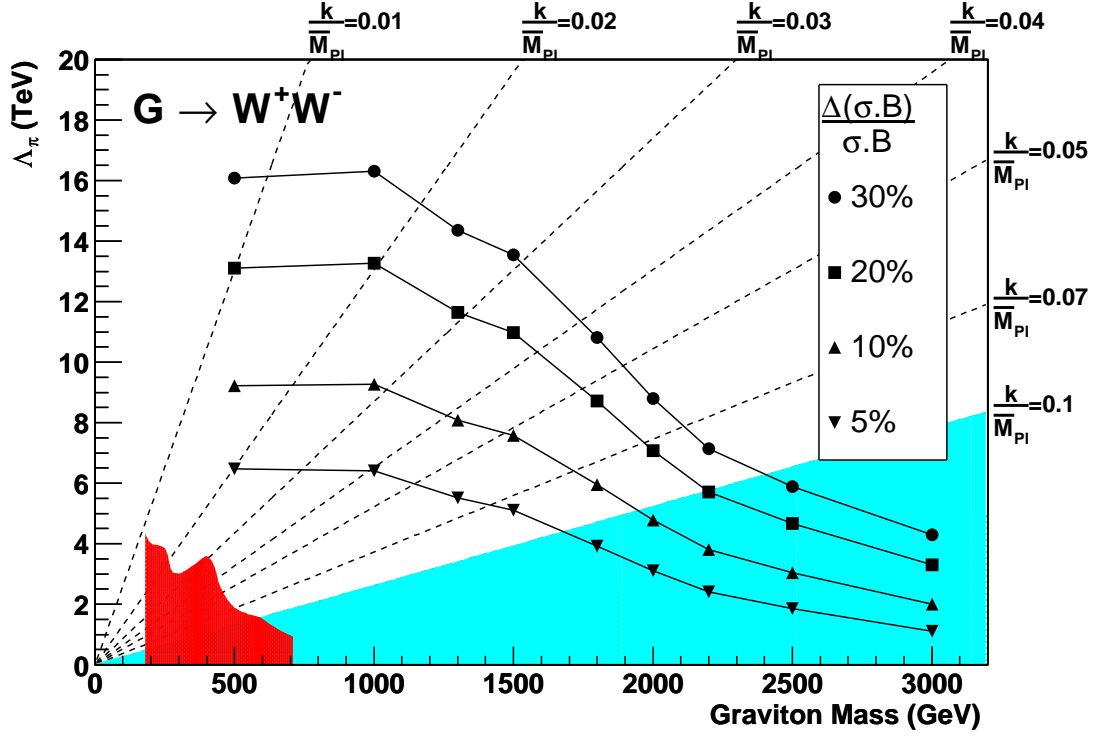
Figure 10: Contours of statistical precision for $\sigma.B$ in the $G \to WW$ channel, as for Figure 6.

is not sufficient for a discovery in this decay channel, it is adequate for measurement of the graviton coupling over much of parameter space; $N_S/\sqrt{N_B}$ varies from 3.8 (for $m_G = 500$ GeV, $k/\overline{M}_{Pl} = 0.02$) to 0.1 (for $m_G = 2200$ GeV, $k/\overline{M}_{Pl} = 0.1$). N_S and N_B are the number of $G \to jj$ signal and background events after the selection cuts.

The mass of the graviton is determined from the invariant mass of the two highest E_T jets; if a third jet is in close proximity ($\Delta\eta, \Delta\phi < 1$) to one of these two high E_T jets, the mass of the graviton is calculated from the invariant mass of the three highest E_T jets. The mass resolution for this decay mode degrades dramatically with a long tail toward lower masses (*e.g.*, the mass resolution is about 160 GeV for a 2000 GeV graviton).

To extract the signal, a procedure independent of the signal shape has been adopted. The mass distribution of the jets is fitted by a Gaussian signal (whose peak is fixed to be at the previously determined peak of the signal) on a background of exponential form. The procedure for subtracting the background under the peak is the same as that for the $G \to WW$ channel. Figure 12b shows the signal after background subtraction. The very high statistics in the background sidebands allow the background under the signal to be estimated with very high precision, revealing the signal peak. Figure 13 shows the fractional error on $\sigma.B$ versus Λ_π and graviton mass in the $G \to jj$ decay mode for 100 fb^{-1} of integrated luminosity.
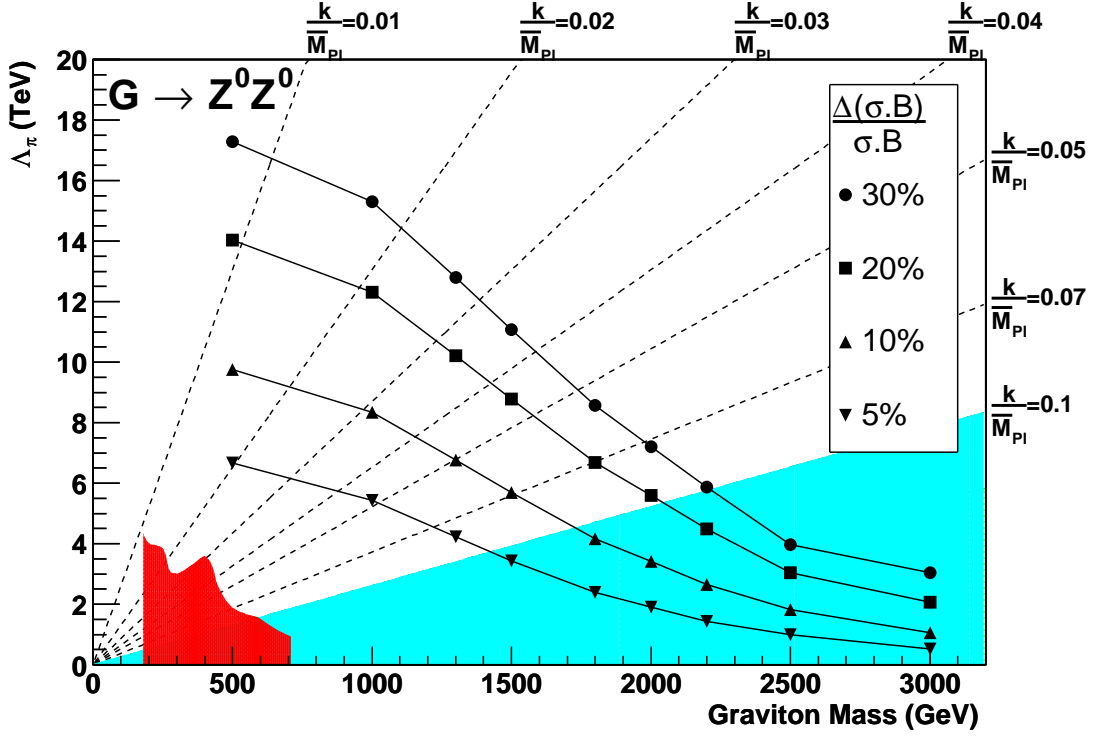
Figure 11: Contours of statistical precision for $\sigma.B$ in the $G \to ZZ$ channel, as for Figure 6.

6.2 Decays to heavy quarks

We have considered whether tagging heavy quarks (t or b) might be useful to improve the signal to background ratio and allow a better measurement of the graviton coupling to quarks. However, since both the graviton and gluon couplings to quarks are flavour independent, no extra discrimination is obtained. The best experimental strategy is therefore to exploit the higher statistical power of the inclusive dijet channel.

7. Decays to Higgs pairs

In the case that $m_G > 2m_H$ then the channel $G \to HH$ is open. The angular distribution is given in Table 1. The branching ratio is 1/12 of that into di-photons, if $m_G \gg 2m_H$. The dominant final state will be 4 b-quarks (for a light Higgs boson) or 4 W's (for a heavy Higgs boson). Both of these final states are difficult to reconstruct, and will have poor statistics. The Higgs coupling is therefore unlikely to be measurable at the LHC.

8. Summary of the reach for coupling measurements

The results of the simulations of each graviton decay channel are summarised in Table 2. The precision which can be reached on $\sigma.B$ in each of the channels investigated, is presented for a range of points in the m_G, Λ_π plane.
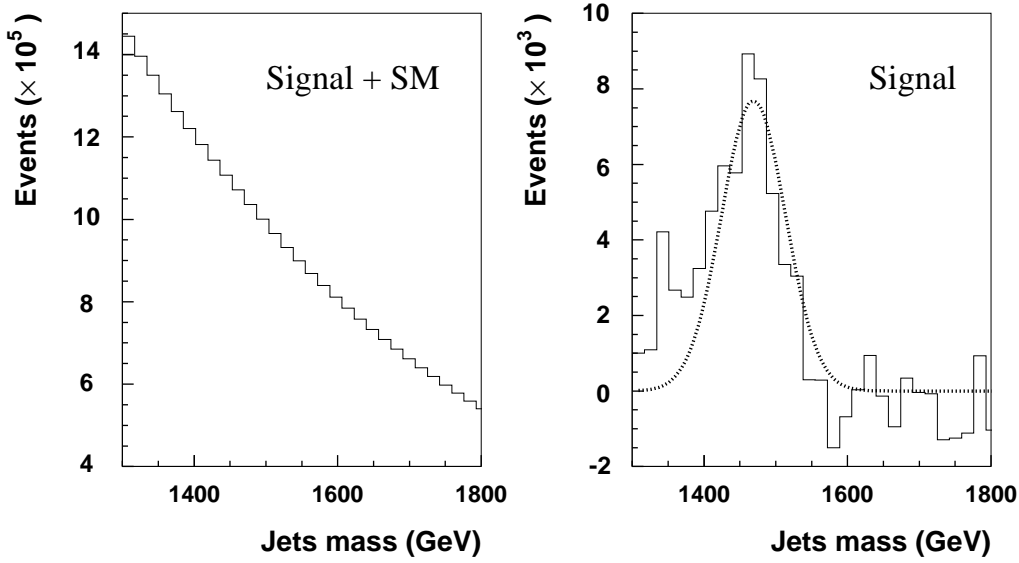
Figure 12: Distribution of invariant mass a) for all two jet events selected, and b) after background subtraction.

	Point m_G, Λ_π (TeV)							
Channel	1,10	1,20	1,30	2,10	2,20	2,30	3,10	3,20
e^+e^-	1.6	3.3	5.3	5.4	11.0	17.1	15.1	30.7
$\mu^+\mu^-$	1.9	4.5	8.2	6.2	15.2	28.2	15.1	32.7
$\gamma\gamma$	1.2	2.9	5.2	3.9	8.8	15.2	10.5	23.0
WW	11.6	44.9	-	38.2	-	-	-	-
ZZ	13.7	50.1	-	52.7	-	-	-	-
jj	19.0	77.0	-	31.0	-	-	59.0	-

Table 2: The relative precision achievable (in %) for measurements of $\sigma.B$ in each of the channels considered, for fixed points in the m_G, Λ_π plane. Points with errors above 100% are not shown.

9. Determination of the model parameters

Several models have been built [9, 10] in which our analysis applies. They are based on the original RS model but with additional branes. Supersymmetric versions [14, 15] have also been constructed, in which the graviton resonances are identical to the ones studied here. These models all have a narrow relatively strongly coupled first massive graviton mode,
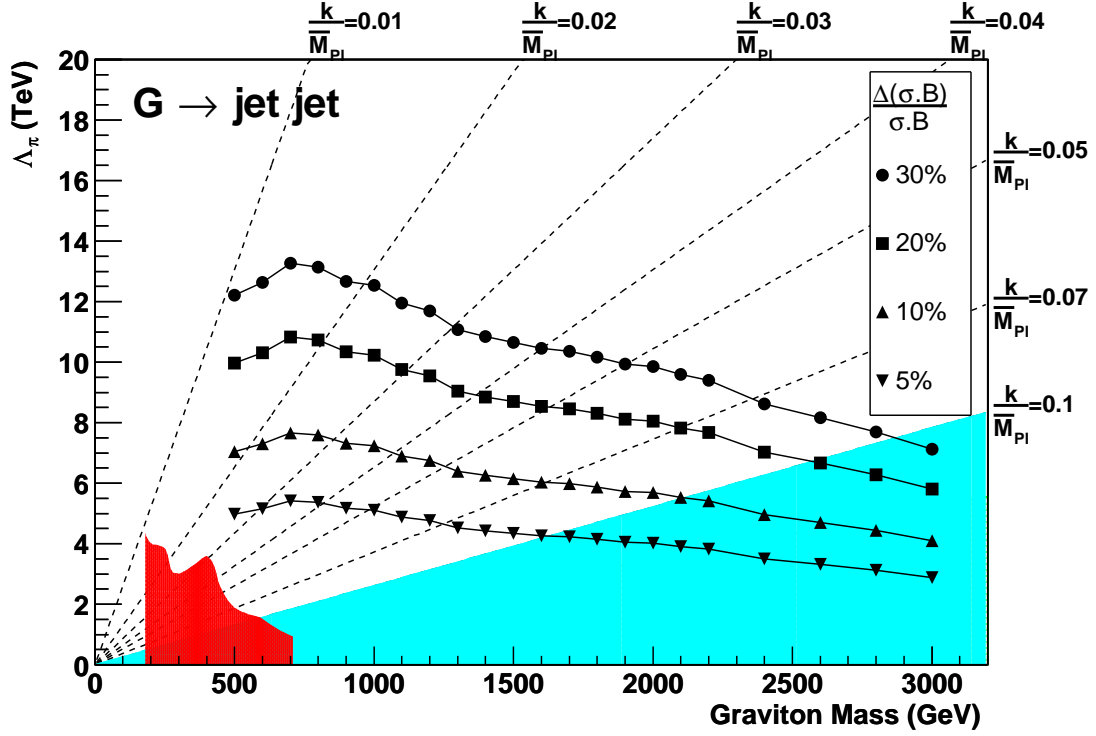
Figure 13: The fractional error on $\sigma.B$ versus Λ_π and graviton mass in $G \rightarrow jj$ decay mode for 100 fb^{-1} of integrated luminosity, as for Figure 6.

and our analysis should apply to them (as long as the parameters are such that the graviton is narrower than the experimental resolution). This is because graviton modes couple to matter in proportionality to the energy-momentum tensor as a model-independent feature, guaranteeing the universality of the coupling. The overall coupling strength is a model dependent parameter, as of course is the connection between the model parameters and the mass or coupling of the first graviton mode. We note that even in the factorisable extra dimension case [22, 23], the resonances would be well separated if the extra dimension were small enough. The splitting between the resonances in the factorisable case is constant, being $2\pi/R$ where R measures the size of the extra dimension(s) [30]. If $1/R$ were in the range $M_Z - 1$ TeV, resonance graviton production would still not be possible because each state couples with negligible strength, suppressed by the Planck mass. But if models were constructed which increase this coupling in the factorisable dimension scenario, our analysis would be fully applicable to this case also.

As a specific example, we have considered the precision which could be obtained on the parameters of the RS model, in the case $m_G = 1500$ GeV. Since the model only contains two parameters (m_G and $\Lambda_\pi = 39$ TeV), only two measurements are required to fully constrain the model. m_G can be measured directly in the e^+e^- channel, with a statistical precision of better than 1 GeV (our fit gives 0.7 GeV for $m_G = 1500$ GeV). The energy scale error is given in [36] as $< 0.7\%$ in this energy range, giving a resolution on m_G of

10.5 GeV. The statistical error on the coupling depends on Λ_π, ranging from 1% at low Λ_π to 15% for Λ_π=39 TeV as in the test model. The dominant systematic error on the coupling is due to the luminosity measurement, since the systematic errors on efficiencies and acceptances will be below the 1% level. We assume, conservatively, that the luminosity can be obtained to 10%, giving an overall error on $\sigma.B$ of 18%. We can then infer a value for the compactification radius of the extra dimension, r_c, and its error, using equations (1.1) and (1.2). The precision on the coupling measurement is then directly reflected in the error in r_c giving $r_c = (82 \pm 7) \times 10^{-33}$ m. This reach to extremely small distance scales is a consequence of the warp factor in the model, working on the TeV-scale measurements of physical observables.

10. Conclusions

The LHC detectors will be capable of discovering narrow graviton resonances predicted in a range of models with extra space dimensions. Such resonances will most easily be detected in the di-electron and di-photon final states. The coupling strength of the resonance to $\mu^+\mu^-, W^+W^-, Z^0Z^0$ and jet–jet final states (but not $\tau^+\tau^-$ or H^0H^0) can also be measured over a wide range of parameter space. The resonance spin can also be measured over a more limited mass range. Taken together, these measurements would provide compelling evidence for the existence of a massive graviton resonance coupling to the SM fields with a universal coupling strength.

Since models with a small number of Planck-scale extra dimensions are highly constrained, the model parameters can be extracted with good precision, if a particular scenario is assumed. In the RS test model, the size of the extra dimension can be inferred to better than 10%, corresponding to a precision in length of 7×10^{-33} m, using measurements of $\sigma.B$ and the graviton mass.

References

[1] L. Randall and R. Sundrum, *A large mass hierarchy from a small extra dimension*, *Phys. Rev. Lett.* **83** (1999) 3370–3373, [http://arXiv.org/abs/hep-ph/9905221].

[2] L. Randall and R. Sundrum, *An alternative to compactification*, *Phys. Rev. Lett.* **83** (1999) 4690–4693, [http://arXiv.org/abs/hep-th/9906064].

[3] C. Csaki and Y. Shirman, *Brane junctions in the Randall-Sundrum scenario*, *Phys. Rev.* **D61** (2000) 024008, [http://arXiv.org/abs/hep-th/9908186].

[4] J. Lykken and L. Randall, *The shape of gravity*, *JHEP* **06** (2000) 014, [http://arXiv.org/abs/hep-th/9908076].

[5] I. Oda, *Mass hierarchy from many domain walls*, *Phys. Lett.* **B480** (2000) 305–311, [http://arXiv.org/abs/hep-th/9908104].

[6] I. Oda, *Mass hierarchy and trapping of gravity*, *Phys. Lett.* **B472** (2000) 59–66, [http://arXiv.org/abs/hep-th/9909048].

[7] T.-j. Li, *Non-compact AdS(5) universe with parallel positive tension 3-branes*, *Phys. Lett.* **B478** (2000) 307, [http://arXiv.org/abs/hep-th/9911234].

[8] N. Arkani-Hamed, S. Dimopoulos, G. R. Dvali, and N. Kaloper, *Infinitely large new dimensions*, *Phys. Rev. Lett.* **84** (2000) 586–589, [http://arXiv.org/abs/hep-th/9907209].

[9] I. I. Kogan, S. Mouslopoulos, A. Papazoglou, G. G. Ross, and J. Santiago, *A three three-brane universe: New phenomenology for the new millennium?*, *Nucl. Phys.* **B584** (2000) 313–328, [http://arXiv.org/abs/hep-ph/9912552].

[10] I. I. Kogan, S. Mouslopoulos, A. Papazoglou, and G. G. Ross, *Multi-brane worlds and modification of gravity at large scales*, *Nucl. Phys.* **B595** (2001) 225–249, [http://arXiv.org/abs/hep-th/0006030].

[11] V. A. Rubakov, *Large and infinite extra dimensions: An introduction*, *Phys. Usp.* **44** (2001) 871–893, [http://arXiv.org/abs/hep-ph/0104152].

[12] W. D. Goldberger and M. B. Wise, *Modulus stabilization with bulk fields*, *Phys. Rev. Lett.* **83** (1999) 4922–4925, [http://arXiv.org/abs/hep-ph/9907447].

[13] R. Altendorfer, J. Bagger, and D. Nemeschansky, *Supersymmetric Randall-Sundrum scenario*, *Phys. Rev.* **D63** (2001) 125025, [http://arXiv.org/abs/hep-th/0003117].

[14] T. Gherghetta and A. Pomarol, *Bulk fields and supersymmetry in a slice of AdS*, *Nucl. Phys.* **B586** (2000) 141–162, [http://arXiv.org/abs/hep-ph/0003129].

[15] T. Gherghetta and A. Pomarol, *A warped supersymmetric standard model*, *Nucl. Phys.* **B602** (2001) 3–22, [http://arXiv.org/abs/hep-ph/0012378].

[16] W. D. Goldberger, Y. Nomura, and D. R. Smith, *Warped supersymmetric grand unification*, http://arXiv.org/abs/hep-ph/0209158.

[17] B. C. Allanach, K. Odagiri, M. A. Parker, and B. R. Webber, *Searching for narrow graviton resonances with the ATLAS detector at the Large Hadron Collider*, *JHEP* **09** (2000) 019, [http://arXiv.org/abs/hep-ph/0006114].

[18] P. Traczyk and G. Wrochna, *Search for Randall-Sundrum graviton excitations in the CMS experiment*, http://arXiv.org/abs/hep-ex/0207061.

[19] H. Davoudiasl, J. L. Hewett, and T. G. Rizzo, *Bulk gauge fields in the Randall-Sundrum model*, *Phys. Lett.* **B473** (2000) 43–49, [http://arXiv.org/abs/hep-ph/9911262].

[20] H. Davoudiasl, J. L. Hewett, and T. G. Rizzo, *Experimental probes of localized gravity: On and off the wall*, *Phys. Rev.* **D63** (2001) 075004, [http://arXiv.org/abs/hep-ph/0006041].

[21] H. Davoudiasl, J. L. Hewett, and T. G. Rizzo, *Phenomenology of the Randall-Sundrum gauge hierarchy model*, *Phys. Rev. Lett.* **84** (2000) 2080, [http://arXiv.org/abs/hep-ph/9909255].

[22] N. Arkani-Hamed, S. Dimopoulos, and G. R. Dvali, *The hierarchy problem and new dimensions at a millimeter*, *Phys. Lett.* **B429** (1998) 263–272, [http://arXiv.org/abs/hep-ph/9803315].

[23] I. Antoniadis, N. Arkani-Hamed, S. Dimopoulos, and G. R. Dvali, *New dimensions at a millimeter to a fermi and superstrings at a tev*, *Phys. Lett.* **B436** (1998) 257–263, [http://arXiv.org/abs/hep-ph/9804398].

[24] E. Accomando, I. Antoniadis, and K. Benakli, *Looking for TeV-scale strings and extra-dimensions*, *Nucl. Phys.* **B579** (2000) 3–16, [http://arXiv.org/abs/hep-ph/9912287].

[25] I. Antoniadis, K. Benakli, and M. Quiros, *Direct collider signatures of large extra dimensions*, *Phys. Lett.* **B460** (1999) 176–183, [http://arXiv.org/abs/hep-ph/9905311].

[26] L. Vacavant and I. Hinchliffe, *Model independent extra-dimension signatures with ATLAS*, http://arXiv.org/abs/hep-ex/0005033.

[27] G. Corcella *et. al.*, *HERWIG 6: An event generator for hadron emission reactions with interfering gluons (including supersymmetric processes)*, *JHEP* **01** (2001) 010, [http://arXiv.org/abs/hep-ph/0011363].

[28] G. Corcella *et. al.*, *HERWIG 6.4 release note*, http://arXiv.org/abs/hep-ph/0201201.

[29] E. Richter-Was, D. Froidevaux, and L. Poggioli, *ATLFAST 2.0: a fast simulation package for ATLAS*, *ATLAS Internal Note* (1998) ATL–PHYS–98–131.

[30] G. F. Giudice, R. Rattazzi, and J. D. Wells, *Quantum gravity and extra dimensions at high-energy colliders*, *Nucl. Phys.* **B544** (1999) 3–38, [http://arXiv.org/abs/hep-ph/9811291].

[31] T. Han, J. D. Lykken, and R.-J. Zhang, *On Kaluza-Klein states from large extra dimensions*, *Phys. Rev.* **D59** (1999) 105006, [http://arXiv.org/abs/hep-ph/9811350].

[32] J. F. Owens, *An updated set of parton distribution parametrizations*, *Phys. Lett.* **B266** (1991) 126–130.

[33] A. D. Martin, R. G. Roberts, W. J. Stirling, and R. S. Thorne, *Scheme dependence, leading order and higher twist studies of MRST partons*, *Phys. Lett.* **B443** (1998) 301–307, [http://arXiv.org/abs/hep-ph/9808371].

[34] G. Corcella *et. al.*, *HERWIG 6.3 release note*, http://arXiv.org/abs/hep-ph/0107071.

[35] R. S. Thorne, *Private communication*, .

[36] **ATLAS** Collaboration, *Detector and physics performance technical design report*, *CERN/LHCC* (1999) 99–15.

[37] **CDF** Collaboration, F. Abe *et. al.*, *Limits on quark-lepton compositeness scales from dileptons produced in 1.8-tev p anti-p collisions*, *Phys. Rev. Lett.* **79** (1997) 2198–2203.

[38] **D0** Collaboration, B. Abbott *et. al.*, *Measurement of the high-mass drell-yan cross section and limits on quark-electron compositeness scales*, *Phys. Rev. Lett.* **82** (1999) 4769–4774, [http://arXiv.org/abs/hep-ex/9812010].

[39] **CDF** Collaboration, F. Abe *et. al.*, *Measurement of the cross-section for production of two isolated prompt photons in anti-p p collisions at s**(1/2) = 1.8-tev*, *Phys. Rev. Lett.* **70** (1993) 2232–2236.

[40] K. Sridhar, *Constraining the randall-sundrum model using diphoton production at hadron colliders*, *JHEP* **05** (2001) 066, [http://arXiv.org/abs/hep-ph/0103055].

[41] R. Bonciani, S. Catani, M. L. Mangano, and P. Nason, *NLL resummation of the heavy-quark hadroproduction cross-section*, *Nucl. Phys.* **B529** (1998) 424–450, [http://arXiv.org/abs/hep-ph/9801375].

[42] W. T. Giele, T. Matsuura, M. H. Seymour, and B. R. Webber, *W boson plus multijets at hadron colliders: HERWIG parton showers versus exact matrix elements*, . Contribution to Proc. of 1990 Summer Study on High Energy Physics: Research Directions for the Decade, Snowmass, CO, Jun 25 - Jul 13, 1990.

[43] I. C. Park, *A new showering algorithm: Mulguisin*, *ATLAS Internal Communication* (1999) ATL–COM–PHYS–99–055.